Unlocking Metal-Ligand Cooperative Catalytic Photochemical Benzene Carbonylation: A Mechanistic Approach

Francesco Crisanti[a], Michael Montag[b], David Milstein[b], Julien Bonin[a,*] and Niklas von Wolff[a,*]

[a] Université Paris Cité, CNRS, Laboratoire d'Electrochimie Moléculaire (LEM), F-75013, Paris, France

[b] Department of Molecular Chemistry and Materials Science, The Weizmann Institute of Science, Rehovot, 76100, Israel

KEYWORDS. Benzene Carbonylation, Photocatalysis, C-H Activation, Metal-Ligand Cooperation, Reaction Mechanisms

ABSTRACT: A key challenge in green synthesis is the catalytic transformation of renewable substrates at high atom and energy efficiency, with minimal exergonicity (ΔG≈0). Non-thermal pathways, i.e., electrochemical and photochemical, can be used to leverage renewable energy resources to drive chemical processes at well-defined energy input and efficiency. Within this context, photochemical benzene carbonylation to produce benzaldehyde is a particularly interesting, albeit challenging, process that combines unfavorable thermodynamics (ΔG° = 1.7 kcal/mol) and the breaking of strong C-H bonds (113.5 kcal/mol) with full atom efficiency and renewable starting materials. Nevertheless, little progress has been made since this transformation was first reported, in 1980s and '90s. By following a mechanistic approach, applying spectrophotochemical and computational tools, we sought to gain a detailed understanding of the non-thermal C-H activation of benzene using metal-ligand cooperative (MLC) PNP rhodium complexes. This allowed us to unlock catalytic MLC benzene carbonylation promoted by irradiation in the near-visible UV region (390 nm) for the first time.

INTRODUCTION

For the chemical sector to achieve the goal of net-zero carbon emission, it is crucial to increase the energetic efficiency of chemical processes, to improve their atom economy, and to make extensive use of renewable resources, in accordance with green chemistry principles and projected roadmaps.[1–3] In an ideal scenario, a desired product would be generated catalytically from renewable feedstocks at full atom efficiency, with minimal and renewable energy input (ΔG≈0). In this respect, both electrochemical and photochemical approaches are desirable, as they allow for a controlled, measurable and sustainable energy input (*via* the applied potential or chosen wavelength). Over the last decades, electrocatalysis has evolved as a tool to transform renewable substrates (e.g., CO_2) at minimal overpotential,[4–8] while catalytic photochemical processes have been used to leverage highly atom-efficient C-H bond activation for the construction of molecular complexity.[9–15] In recent years, it was shown that both electrochemical and photochemical approaches can produce CO from CO_2 at high rate and with excellent selectivity,[16–18] making it a valuable and renewable C_1-builduing block. While a plethora of carbonylative C-H transformations exists,[19–24] we are interested in applying photo- and electrochemical approaches to enable otherwise endergonic processes *via* the use of these renewable energy inputs. Within this context, the photochemical carbonylation of benzene to produce benzaldehyde is particularly interesting, as it combines two renewable[25,26] and non-functionalized substrates into an interesting platform chemical at full atom efficiency.[27] Benzene carbonylation is indeed highly challenging, due to unfavorable thermodynamics (ΔG° = 1.7 kcal/mol) and the strong benzene C-H bond (113.5 kcal/mol), and thus serves as an ideal testing ground for novel non-thermal catalytic approaches. However, since the initial reports on rhodium-catalyzed photochemical benzene carbonylation were published, in the late 1980s and early 1990s, little progress has been made in this field.[28–33] In recent work, we showed that non-thermal, electrochemical pathways can be used to activate metal-ligand cooperative (MLC)[34–36] catalysts for endergonic dehydrogenation reactions at room temperature.[37,38] This prompted us to explore whether non-thermal MLC chemistry could also be leveraged for catalytic benzene carbonylation. Following a mechanistic approach, we seek to identify, understand and overcome bottlenecks in photochemical carbonylative C-H activation promoted by MLC systems, with the goal of providing novel alternatives for catalytic benzene carbonylation.

Despite the elegance of benzene carbonylation, which allows benzaldehyde, an important molecular building block, to be synthesized in a single step from simple and renewable feedstocks,[25] the widespread application of this process is hampered by unfavorable thermodynamics and the low productivity of most catalysts employed for this reaction. Early work by Kunin and Eisenberg showed that a rhodium-

based Vaska-type complex, *trans*-[Rh(CO)Cl(PPh$_3$)], can catalyze this reaction, achieving a turnover number (TON) of 2.1 after 40 h of irradiation (Hg/Xe arc, 200 W).[33] In their report, the authors demonstrated the role of light in overcoming kinetic barriers, and the system was also found to be very competent in promoting the reverse process, i.e., photochemical benzaldehyde decarbonylation. Nevertheless, although under irradiation the forward reaction could proceed at room temperature, the system was limited by the low equilibrium concentration of benzaldehyde, governed by unfavorable thermodynamics. Using a similar system, the PMe$_3$-analogue *trans*-[Rh(CO)Cl(PMe$_3$)], the groups of Tanaka[39] and Goldman[40] demonstrated that the thermodynamic limitation could be overcome, attaining a TON of 48 (60 h) and 52 (24 h, 500 W, Hg-arc lamp), respectively. Thus, changing the phosphine ligand clearly affects the behavior of the catalyst under light, and it appears that the PMe$_3$ variant is able to supply sufficient driving force to overcome the thermodynamic constraints. The non-thermal, photochemical activation of these systems is somewhat reminiscent of recent developments involving the use of electrochemical activation to surmount thermodynamic and kinetic barriers in alcohol dehydrogenation by MLC systems.[41,42]

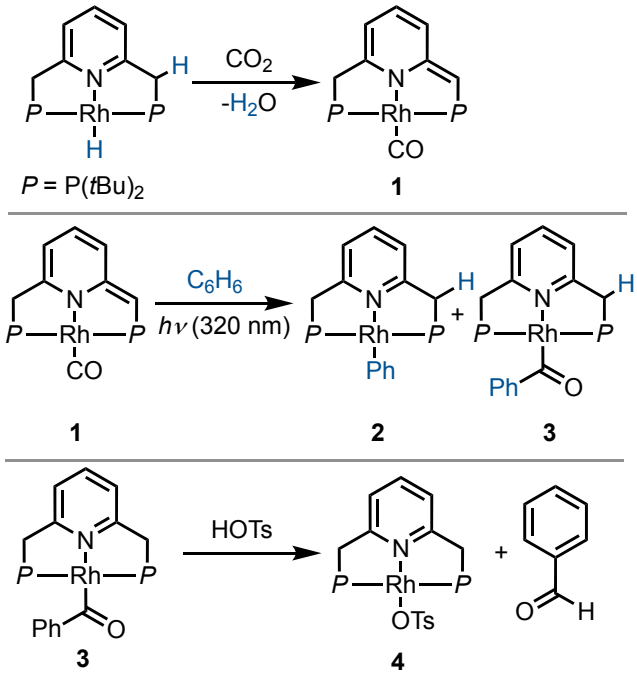

Scheme 1. Reaction of a PNP-rhodium hydride pincer complex with CO_2 and subsequent C-H activation under UV irradiation.

In 2016, The Milstein group reported the photochemical activation of a PNP-rhodium pincer complex, as part of a sequence of reactions that converted benzene and CO_2 into benzaldehyde (Scheme 1).[43] In the initial step, a PNP-rhodium(I) hydride complex was shown to participate in a formal reverse water-gas shift reaction upon treatment with CO_2, generating a dearomatized rhodium(I) carbonyl complex (**1**) and water. In this reaction, a pincer side-arm C-H proton, together with the hydride ligand, are involved in the cleavage of a C=O bond of CO_2. Interestingly, under UV irradiation (λ_{max} = 320 nm), complex **1** was found to promote the C-H activation of benzene *via* metal-ligand cooperativity, to form the corresponding acyl complex **3**. Treatment of the latter with tosylic acid released benzaldehyde with co-formation of the tosylate complex **4**. Addition of base and H_2 to this complex regenerated the initial Rh(I)-hydride complex, thereby closing a stoichiometric cycle for benzaldehyde formation from benzene and CO_2. Given the photochemical activation of benzene by **1**, and the possibility of releasing benzaldehyde, albeit under acidic conditions, we attempted direct benzene carbonylation under UV irradiation using **1** as catalyst, achieving limited success, with TON = 1.3 after 120 h. Similarly, a rhodium MLC PN^{3}P-complex was used by Huang and co-workers for the stoichiometric carbonylation of benzene under thermal conditions, using hydrochloric acid for benzaldehyde release.[44] Inspired by these preliminary results, we sought to understand the mechanism of this reaction in greater detail, in order to determine its limiting steps, and probe the conditions under which light can serve as a driving force for significant product formation. This would open the door for the use of MLC systems for catalytic benzene carbonylation, which has yet to be achieved. To this end, several aspects of a potential catalytic cycle have to be understood: (i) What is the role of light in the C-H activation step? (ii) Is benzene carbonylation by MLC complexes an associative process (as in the work of Tanaka and Goldman) or a dissociative one (as proposed by Kunin and Eisenberg)? (iii) How can benzaldehyde be released from the catalyst in order to close the catalytic cycle?

RESULTS AND DISCUSSION

We first investigated the behavior of different PNP-rhodium pincer complexes towards benzene C-H activation in the absence of carbon monoxide gas (Scheme 2). Complex **1**, bearing the strongly-coordinated CO ligand *trans* to the lutidine core, does not activate benzene C-H bonds in the dark, i.e., it slowly decomposes in neat benzene over the course of two weeks at room temperature, but does not form phenyl complex **2** or acyl complex **3**. By contrast, dearomatized PNP-rhodium complexes bearing more weakly coordinated ligands, namely, N_2,[45] chloride (Cl^-)[46] or triflate (OTf^-),[45] react with benzene in the dark, with the time required to complete this reaction decreasing from 4 d to 9 h to 1 h, respectively. The reactivity of these dearomatized pincer complexes towards C-H activation is thus inversely correlated with metal-ligand bonding strength (CO > N_2 > Cl^- > OTf^-). Based on this observation, our initial hypothesis was that a transiently formed three-coordinate 14e Rh(I) species is responsible for C-H activation, as proposed for the system reported by Kunin and Eisenberg.[29] In complex **1**, the strongly bonded CO ligand would prevent the formation of the transient, coordinatively unsaturated species in the dark, hence explaining its lack of reactivity in the absence of light.

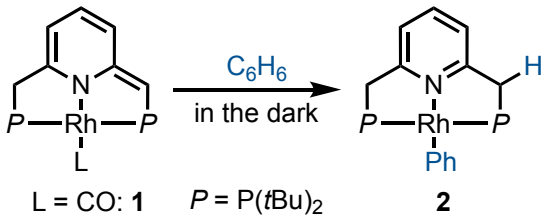

L = CO: no reaction
L = N_2: 96 h
L = Cl^-: 9 h (anionic complex)
L = OTf^-: 1 h (anionic complex)

Scheme 2. Rate of benzene C-H activation by different neutral and anionic PNP-rhodium(I) pincer complexes, as reflected in the approximate time to reaction completion.

To further probe this hypothesis, we examined the CO self-exchange rates of complex **1** in the dark and under irradiation. In a sealed J. Young NMR tube, a 2 mM solution of unlabeled complex **1** [**1(**^{12}**CO)**] in 7:1 *n*-heptane:cyclohexane-d_{12} was placed under 1 atm of ^{13}CO, and the CO ligand exchange was monitored by ^{31}P{^{1}H} NMR spectroscopy. In the dark, at room temperature, ^{13}CO incorporation was observed within a few minutes, as clearly evidenced by the appearance of ^{31}P-^{13}C coupling ($^2J_{P\text{-}C}$ = 12.7 Hz) in the corresponding NMR peaks (Figure 1a). The same experiment was repeated at -40 °C (Figure 1b), showing roughly 75% ^{13}CO incorporation after 4 h. These results show that CO lability is high in the absence of irradiation on the timescale of photocatalysis. From the NMR spectra, it is apparent that immediate incorporation of ^{13}CO takes place even in the absence of irradiation. This suggests that (i) CO self-exchange is very rapid at room temperature, and (ii) light is not needed for this step. However, this does not rule out the involvement of a three-coordinate intermediate responsible for C-H activation. Having shown that putative three-coordinate species can quickly generate the rhodium phenyl complex **2** (Scheme 2), we wanted to know whether this complex could be an intermediate en route to the acyl species **3**, potentially leading to the release of benzaldehyde.

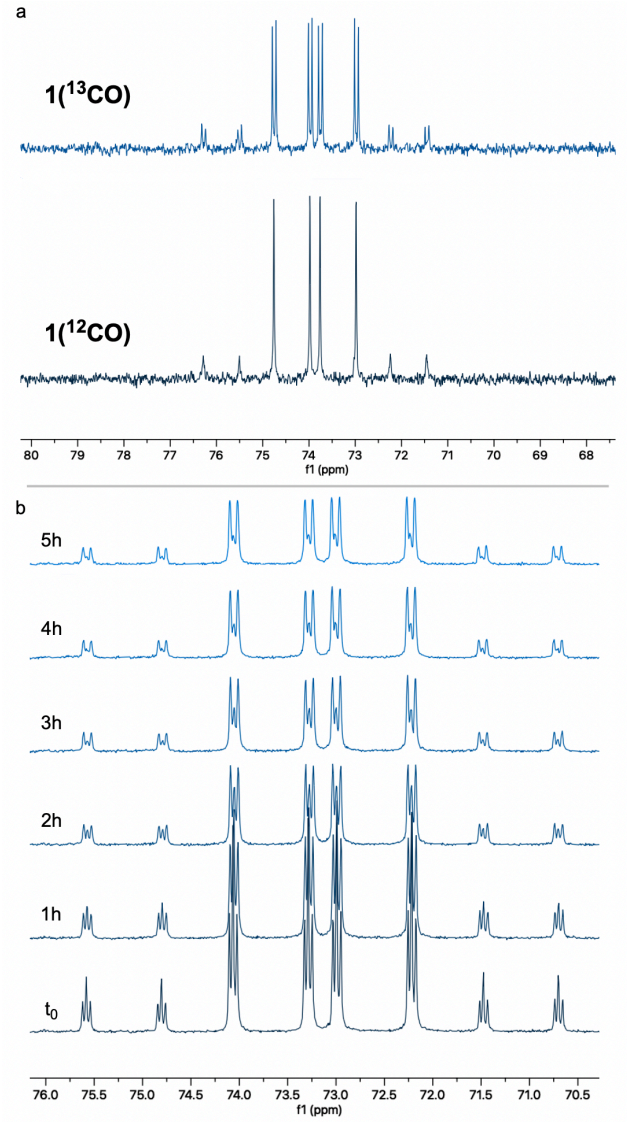

Figure 1. a) CO self-exchange in a 2 mM solution of **1(¹²CO)** in 7:1 *n*-pentane/cyclohexane-d_{12} under 1 atm of ^{13}CO, as observed by $^{31}P\{^{1}H\}$ NMR spectroscopy in the dark at room temperature. b) Low temperature (-40 °C) $^{31}P\{^{1}H\}$ NMR monitoring of such CO self-exchange in the same solvent mixture (all spectra represent mixtures of **1(¹²CO)** and **1(¹³CO)** at varying ratios).

When a benzene solution of **2** was placed under 1 atm of CO, this complex converted over the course of several minutes (the time to run an NMR-spectrum) into **3** at room temperature, in the dark, as observed by $^{31}P\{^{1}H\}$ NMR spectroscopy (Figure 2). CO insertion into the Rh-Ph bond is thus a facile, non-photochemical process. While it was initially thought that externally-added acid is necessary for the release of benzaldehyde from **3**, we wanted to understand whether this could instead be triggered by light or CO coordination.[40,42] To explore potential CO-induced benzaldehyde release, we used UV-visible absorption spectroscopy to monitor the reaction of a 30 μM solution of **3** under CO at room temperature (Figure 3), employing pentane as solvent in order to avoid benzene C-H activation as a side-reaction. After 55 min under 1 atm of CO, the reaction mixture showed the characteristic absorption bands of complex **1**, with spectral deconvolution giving an excellent fit to a mixture of **1** and **3** (Figure 4). ^{1}H NMR spectroscopy revealed the concomitant formation of benzaldehyde under these conditions [see Supporting Information (SI), section 2.8], thereby confirming the successful elimination of the product in the presence of CO. These results clearly indicate that CO can promote benzaldehyde release from **3**, while regenerating **1** through a non-photochemical pathway. Spectral deconvolution over time allowed us to calculate an approximate pseudo first-order rate constant of 9.6×10^{-5} s^{-1} for the reaction **3** + CO → **1** + PhCHO (see SI, section 7), in line with a thermally activated rate-determining step at room temperature. Having established that benzaldehyde release and concurrent formation of **1** can be thermally facilitated by CO, thus potentially closing the catalytic cycle, we turned our attention to

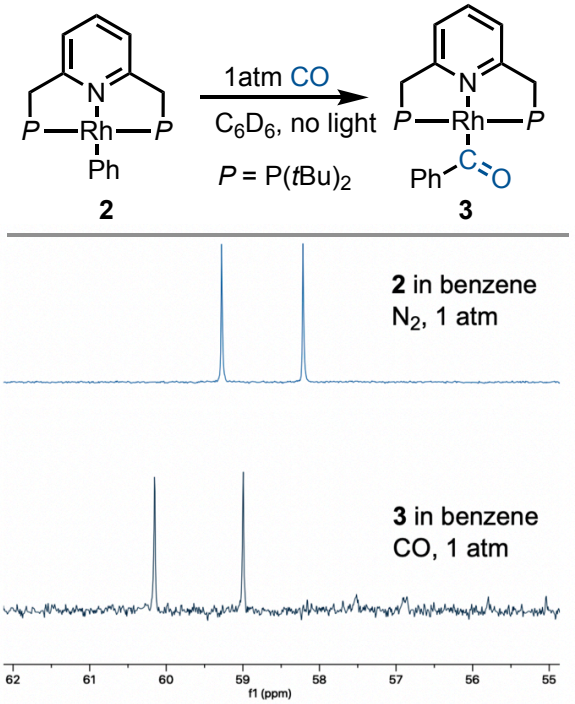

the role of light in the initial C-H activation step. Importantly, our aim was to determine whether this process is associative or dissociative, and to probe the effect of light on its thermodynamics and kinetics.

Figure 2. CO insertion into the Rh-Ph bond of **2** to form **3**, and the consequent changes in the $^{31}P\{^{1}H\}$ NMR spectrum.

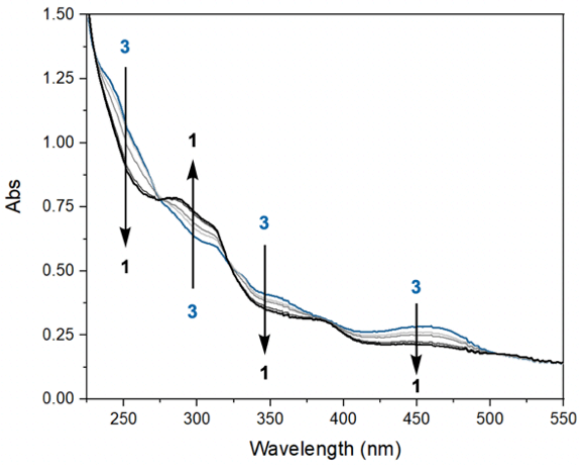

Figure 3. UV-visible spectral evolution of a 30 μM solution of **3** in pentane under 1 atm of CO, at room temperature in the absence of irradiation, over the course of 1 h.

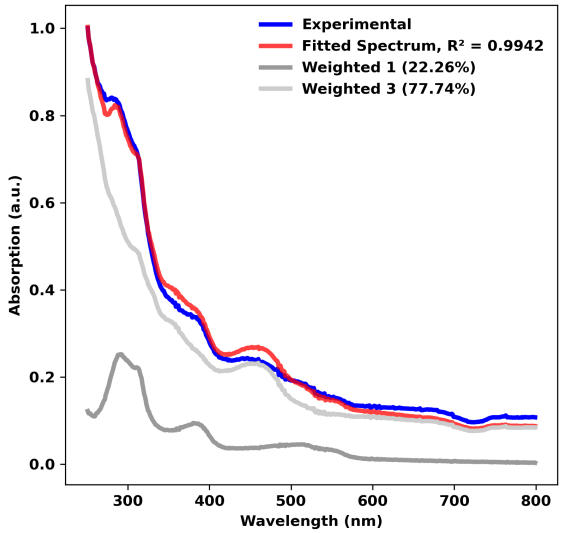

Figure 4. Spectral deconvolution of the UV-visible spectrum of **3** in pentane under 1 atm of CO, recorded after 55 min at room temperature in the absence of irradiation. The UV-visible spectra of **1** and **3** are shown for reference.

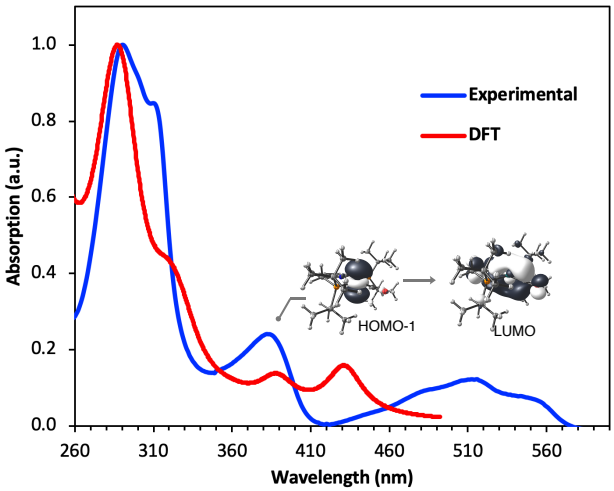

Figure 5. Overlay of the experimental and TD-DFT-derived (see SI for details) UV-visible spectra of complex **1** in pentane. The band at ~390 nm can be assigned to a HOMO-1 (dz^2) → LUMO metal-ligand charge transfer transition.

The UV-visible spectrum of **1** in pentane shows three discernable bands in the UV range: one centered around 280 nm, one around 300 nm and one roughly at 390 nm (Figure 5). Using TD-DFT calculations, we sought to gain insight into the electronic transitions involved in these absorptions. The absorption at ~300 nm seems to be associated with a mixed metal-ligand-based orbital transition, but the one at ~390 nm involves a metal-to-ligand charge transfer (MLCT) transition, with the donor orbital being the Rh d_{z^2} and the acceptor orbital having a Rh-CO antibonding character (Figure 5). This transition resembles the one involved in the mechanism proposed by Goldman and coworkers for *trans*-[Rh(CO)Cl(PMe_3)], in which irradiation depopulates the d_{z^2} orbital, thereby decreasing unfavorable electron-electron repulsions between the rhodium center and benzene substrate.[40]

In the initial report on C-H activation by **1**, a light source with λ_{max} = 320 nm was used.[43] We wanted to investigate whether selectively promoting the MLCT transition at 390 nm could lead to a more active system, by increasing Lewis acidity on the metal center and Lewis basicity on the ligand framework. Starting from **1**, we performed spectrophotochemistry at different temperatures to learn more about the nature of the C-H activation step. A thermostated quartz cuvette containing a 30 μM solution of **1** in benzene under N_2 was placed in a UV-visible spectrophotometer, and was irradiated at 390 nm using a LED light source positioned at a 90° angle with respect to the spectrophotometer beam path, while maintaining the temperature at 20 °C. Under these conditions, the characteristic absorption bands of **1** decreased over time, giving way to the absorption bands of **2** (Figure 6a), with typical isosbestic points, indicating full conversion of **1** into **2**, with concomitant release of CO, over the course of 3 h.

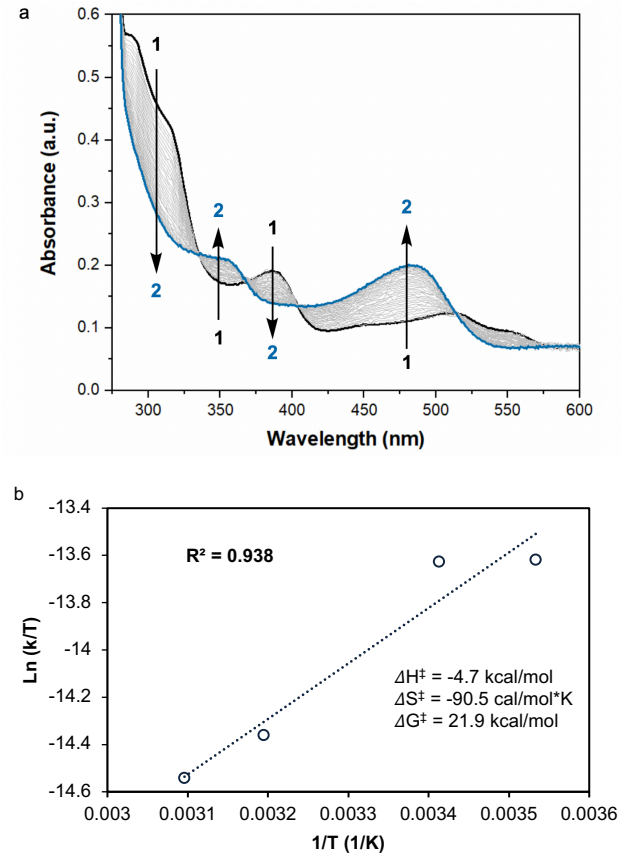

Figure 6. a) UV-visible spectral evolution during C-H activation of benzene by **1** in the absence of added CO (30 μM of **1** in benzene under N_2 at 20 °C, irradiated at 390 nm at 90° relative to spectrophotometer beam). b) Corresponding Eyring plot and derived activation parameters for the C-H activation step.

Discriminating between associative and dissociative mechanisms is difficult when fitting the data to kinetic rate laws, since first order kinetics are expected in both cases (see SI, section 6). Therefore, the reaction kinetics were studied at different temperatures, in order to extract the activation enthalpy and entropy from the corresponding Eyring plot (Figure 6b). The negative values calculated for $\Delta H^{\ddagger}$ and $\Delta S^{\ddagger}$, -4.7 kcal/mol and -90.5 cal/mol·K, are in line with an associative or interexchange mechanism, followed by CO release. It should be noted that relatively small values of $\Delta H^{\ddagger}$ and the large negative value of $\Delta S^{\ddagger}$ measured for the C-H activation step with **1** are usually linked to an interexchange mechanism.[47] This hypothesis seems to be corroborated by the apparent absence of intermediates in the C-H activation reaction (Figure 6), although it is possible that their concentrations fall below the detection limit of our UV-visible spectrometer.

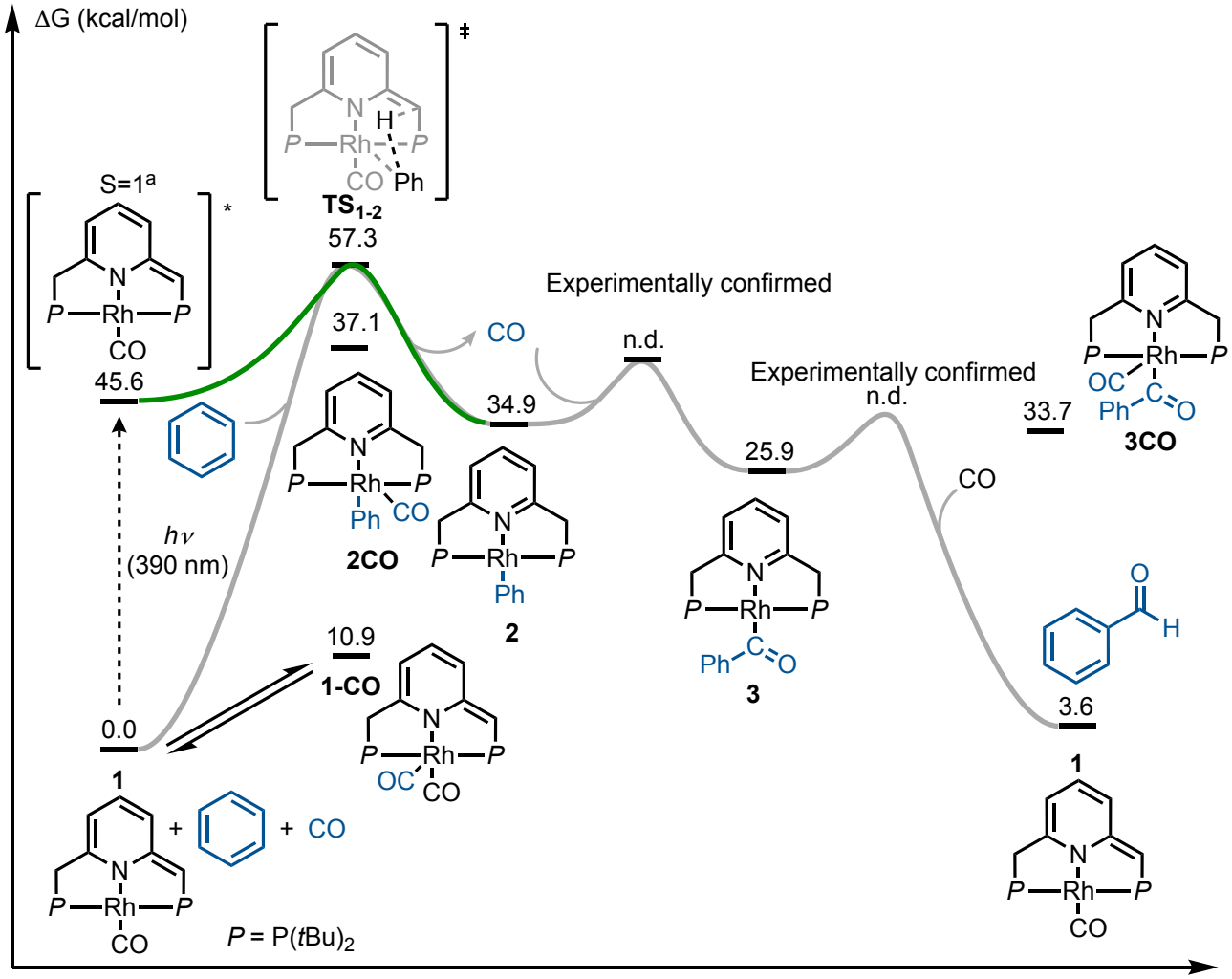

Scheme 3. Potential energy surface for the photochemical carbonylation of benzene catalyzed by 1, calculated at the M06-L/def2VP/W06/GD3/SMD//ωB97M-V/def2TZVPP/RIJCOSX/SMD level of theory. [a]The triplet state was used as a proxy for the geometry of the excited state of the excitation at 390 nm.

In order to better understand the energetics of the different steps comprising the benzene carbonylation reaction catalyzed by **1**, we performed DFT calculations (Scheme 3 and SI, section 8). As one examines the computed reaction profile, several points are immediately evident. The observed and isolated intermediates, namely, **2** and **3**, are strongly uphill energetically compared to the starting material **1**, by about 35 and 26 kcal/mol, respectively. Once **2** is generated, the subsequent steps, including benzaldehyde formation, are strongly exergonic, by as much as 22 kcal/mol. Indeed, we experimentally observed the facile release of benzaldehyde from **2** under CO, with concomitant regeneration of **1** (Figure 3). We propose that irradiation at 390 nm brings complex **1** to an excited state (we used the Gibbs free energy of the triplet state as a proxy for the energy of this excited state, see Scheme 3 and SI section 8.2), which lies 45.6 kcal/mol above the ground state, and that the MLCT character of this transition should increase the Lewis acidity of the metal center and Lewis basicity of the ligand. An associative transition state then leads to C-H activation and subsequent CO release, thereby affording intermediate **2**. Importantly, the observed reaction barrier, $\Delta G^{\ddagger}_{exp}$ = 21.9 kcal/mol (Figure 6), is higher than the computed one, $\Delta G^{\ddagger}_{calc}$(**TS**$_{1\text{-}2}$) = 12.1 kcal/mol (Scheme 3). This could be explained by rovibronic relaxation, as well as triplet-to-singlet intersystem crossing that must take place before reaching the computed transition state, neither of which has been considered in our TD-DFT calculations. The DFT calculations are also helpful in rationalizing the rapid CO self-exchange that occurs in the absence of light. Thus, the pentacoordinate dicarbonyl complex, obtained upon coordination of a second CO ligand to the metal center of **1**, was calculated to be only 10.9 kcal/mol higher in energy than the latter, providing a fast associative process for CO self-exchange. Indeed, associative CO self-exchange pathways involving pentacoordinate rhodium(I) species have been observed in similar systems.[40-41] A dissociative mechanism is less likely, considering the experimentally observed negative $\Delta S^{\ddagger}$ value. Moreover, DFT calculations involving a dissociative/oxidative addition pathway, similar to that proposed by Kunin and Eisenberg, show barriers for C-H activation that are at least 2 kcal/mol higher as compared to the associative **TS**$_{1\text{-}2}$ (see SI, section 8.3), hence disfavoring both CO dissociation from **1** and participation of Rh(III) intermediates.

Table 1. Effect of light source on photochemical benzene carbonylation

Entry	Light source	Power	Wavelength (nm)	TON
1[43]	UVB	80 W	280 < λ < 410	1.3[a]
2	Solar Simulator[b]	100 W	λ > 400	0
3	Solar Simulator[b]	100 W	300 < λ < 1000	4.2±0.3[c]
4	LED	52 W	370 < λ < 410	14.1±1.5[c]

Reaction conditions: 1 mM of **1** in 3 mL of benzene, 1 atm of CO, 72 h irradiation under the cited light source in a quartz cuvette with 3 mL headspace. [a]20 mM of **1**, 1 atm of CO, 120 h irradiation in an NMR tube, 10 x 8 W fluorescent LZC-UVB lamps (Luzchem). [b]100 W Xe lamp. [c]Error corresponds to repeated (> 2) runs.

Having gained a deeper understanding of the benzene carbonylation mechanism, we set to examine whether the mechanistic analysis and identification of the absorption band associated with C-H activation (390 nm) can be translated into higher catalytic activity. As shown previously, irradiation at 320 nm leads to a TON of only 1.3 after 120 h (Table 1, entry 1). Using a solar simulator equipped with a 400 nm bandpass filter, it was found that visible light is insufficient to promote the desired reaction (Table 1, entry 2). Nevertheless, when the same light source was operated without a bandpass filter, more significant benzaldehyde production was observed (~4 TON). Finally, by selectively irradiating the band at 390 nm, using a LED light source, we were able to generate benzaldehyde with an even higher TON of ~14. Thus, by employing **1** as catalyst, and irradiating the reaction mixture at 390 nm, it is possible to drive the carbonylation reaction beyond the low equilibrium concentration of benzaldehyde, i.e., ~2 mM in CO-saturated benzene, and reach a much higher concentration of ~10 mM.

Our successful application of MLC catalysis for photochemical benzene carbonylation shows that, like the electrochemical approach, non-thermal activation pathways can provide the thermodynamic driving force necessary to promote endergonic reactions in a clean and sustainable fashion, without the need for highly reactive co-substrates. The light source is employed as a mono-directional thermodynamic pump to populate high-energy intermediates. The results of our mechanistic experiments are consistent with a light-driven C-H activation step (Scheme 4), followed by a series of thermal steps responsible for product release and catalytic cycle closure. Importantly, CO was shown to be able to promote benzaldehyde release, whereas similar previously-described MLC systems necessitate the use of strong acids to accomplish this step.[44] The presence of a strong acid in an MLC system would ultimately quench the basicity of the ligand, thus preventing successful C-H activation and accounting for the lack of catalytic turnover in such systems. It should also be noted that although intermittent CO release from catalyst **1** is possible, the C-H activation step is associative, indicating that increased CO pressure in a suitable reactor could be beneficial. Such a high-pressure approach could also counter the low solubility of CO in most organic solvents, including benzene (< 10 mM at 1 atm). Finally, our kinetic measurements indicate that thermal activation may still be necessary for accelerating the photochemical benzene carbonylation reaction, as the key light-induced C-H activation step has an activation energy of 21.9 kcal/mol and benzaldehyde release exhibits a low rate constant of 9.6×10^{-5} s^{-1} at room temperature.

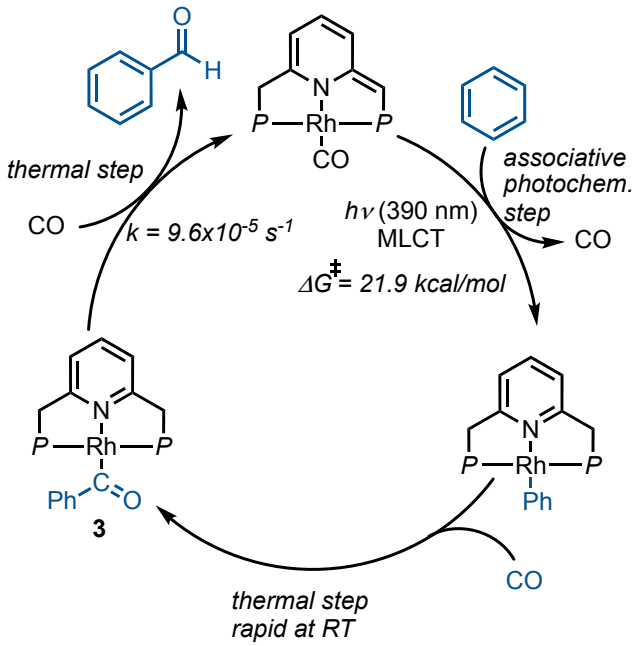

Scheme 4. Proposed catalytic cycle for the photochemical benzene carbonylation promoted by complex **1**.

In summary, photochemical benzene carbonylation *via* C-H activation is a challenging process that has seen little advancement over the last decades, from both a performance and mechanistic point of view. Herein, we demonstrate the unprecedented implementation of MLC catalysis to successfully promote this reaction. Unlocking catalytic carbonylative benzene C-H activation using metal-ligand cooperative catalysts may open novel opportunities in the field. Indeed, preliminary studies conducted in our research group have shown that benzene is not the only substrate that can be functionalized using this type of chemistry. A promising follow-up to this work would be the evaluation of other aromatic substrates, and a comparison of their reactivity.

ASSOCIATED CONTENT

Supporting Information

The Supporting Information, including synthetic procedures, kinetic measurements and information pertaining to DFT calculations, is available free of charge from the ACS Publications website. All computed structures are available free of charge on the ioChem-BD online repository *via* the following link: https://doi.org/10.19061/iochem-bd-6-355

AUTHOR INFORMATION

Corresponding Authors

Julien Bonin – Université Paris Cité, Laboratoire d'Electrochimie Moléculaire, CNRS, F-75013, Paris, France ; orcid.org/0000-0001-9943-0219; julien.bonin@u-paris.fr

Niklas von Wolff – Université Paris Cité, Laboratoire d'Electrochimie Moléculaire, CNRS, F-75013, Paris, France ; orcid.org/0000-0001-8108-5365; niklas.von-wolff@u-paris.fr

Authors

Francesco Crisanti – Université Paris Cité, Laboratoire d'Electrochimie Moléculaire, CNRS, F-75013, Paris, France ; orcid.org/0000-0002-7729-3767

David Milstein – Department of Molecular Chemistry and Materials Science, Weizmann Institute of Science, Rehovot 76100, Israel; orcid.org/0000-0002-2320-0262

Michael Montag – Department of Molecular Chemistry and Materials Science, Weizmann Institute of Science, Rehovot 76100, Israel; orcid.org/0000-0001-6700-1727

Author Contributions

Funding acquisition: N. v. W. Project design: N. v. W. Supervision: N. v. W., J. B., M. M., D. M. Experiments: F.C. DFT calculations: N. v. W. This manuscript was written through contributions from all authors.

ACKNOWLEDGMENT

F. C. warmly acknowledges the IdEx Université de Paris 2021 program for PhD funding, and the Pôle Collège des Ecoles Doctorales of Université Paris Cité for the Bourse Doctorale de Mobilité Internationale that funded his stay at the Weizmann Institute of Science. Computations were performed using HPC resources from GENCI-CINES (Grant AD010812061R2).

REFERENCES

(1) Anastas, P.; Eghbali, N. Green Chemistry: Principles and Practice. *Chem. Soc. Rev.* **2009**, *39* (1), 301–312. https://doi.org/10.1039/B918763B.

(2) *Chemicals – Analysis*. IEA. https://www.iea.org/reports/chemicals (accessed 2022-11-24).

(3) Leech, M. C.; Lam, K. A Practical Guide to Electrosynthesis. *Nat Rev Chem* **2022**, *6* (4), 275–286. https://doi.org/10.1038/s41570-022-00372-y.

(4) Nutting, J. E.; Gerken, J. B.; Stamoulis, A. G.; Bruns, D. L.; Stahl, S. S. "How Should I Think about Voltage? What Is Overpotential?": Establishing an Organic Chemistry Intuition for Electrochemistry. *J. Org. Chem.* **2021**, *86* (22), 15875–15885. https://doi.org/10.1021/acs.joc.1c01520.

(5) Appel, A. M.; Helm, M. L. Determining the Overpotential for a Molecular Electrocatalyst. *ACS Catal.* **2014**, *4* (2), 630–633. https://doi.org/10.1021/cs401013v.

(6) Costentin, C. Molecular Catalysis of Electrochemical Reactions. Overpotential and Turnover Frequency: Unidirectional and Bidirectional Systems. *ACS Catal.* **2021**, 5678–5687. https://doi.org/10.1021/acscatal.1c00744.

(7) Peng, X.; Zeng, L.; Wang, D.; Liu, Z.; Li, Y.; Li, Z.; Yang, B.; Lei, L.; Dai, L.; Hou, Y. Electrochemical C–N Coupling of CO2 and Nitrogenous Small Molecules for the Electrosynthesis of Organonitrogen Compounds. *Chem. Soc. Rev.* **2023**, *52* (6), 2193–2237. https://doi.org/10.1039/D2CS00381C.

(8) Siu, J. C.; Fu, N.; Lin, S. Catalyzing Electrosynthesis: A Homogeneous Electrocatalytic Approach to Reaction Discovery. *Acc. Chem. Res.* **2020**, *53* (3), 547–560. https://doi.org/10.1021/acs.accounts.9b00529.

(9) Grover, J.; Prakash, G.; Goswami, N.; Maiti, D. Traditional and Sustainable Approaches for the Construction of C–C Bonds by Harnessing C–H Arylation. *Nat Commun* **2022**, *13* (1), 1085. https://doi.org/10.1038/s41467-022-28707-9.

(10) Dalton, T.; Faber, T.; Glorius, F. C–H Activation: Toward Sustainability and Applications. *ACS Cent. Sci.* **2021**, *7* (2), 245–261. https://doi.org/10.1021/acscentsci.0c01413.

(11) Campbell, M. W.; Yuan, M.; Polites, V. C.; Gutierrez, O.; Molander, G. A. Photochemical C–H Activation Enables Nickel-Catalyzed Olefin Dicarbofunctionalization. *J. Am. Chem. Soc.* **2021**, *143* (10), 3901–3910. https://doi.org/10.1021/jacs.0c13077.

(12) Oliva, M.; Coppola, G. A.; Van der Eycken, E. V.; Sharma, U. K. Photochemical and Electrochemical Strategies towards Benzylic C–H Functionalization: A Recent Update. *Advanced Synthesis & Catalysis* **2021**, *363* (7), 1810–1834. https://doi.org/10.1002/adsc.202001581.

(13) Zhao, B.; Prabagar, B.; Shi, Z. Modern Strategies for C–H Functionalization of Heteroarenes with Alternative Coupling Partners. *Chem* **2021**, *7* (10), 2585–2634. https://doi.org/10.1016/j.chempr.2021.08.001.

(14) Zhang, L.; Liardet, L.; Luo, J.; Ren, D.; Grätzel, M.; Hu, X. Photoelectrocatalytic Arene C–H Amination. *Nature Catalysis* **2019**. https://doi.org/10.1038/s41929-019-0231-9.

(15) Romero, N. A.; Margrey, K. A.; Tay, N. E.; Nicewicz, D. A. Site-Selective Arene C-H Amination via Photoredox Catalysis. *Science* **2015**, *349* (6254), 1326–1330. https://doi.org/10.1126/science.aac9895.

(16) Ren, S.; Joulié, D.; Salvatore, D.; Torbensen, K.; Wang, M.; Robert, M.; Berlinguette, C. P. Molecular Electrocatalysts Can Mediate Fast, Selective CO_2 Reduction in a Flow Cell. *Science* **2019**, *365* (6451), 367. https://doi.org/10.1126/science.aax4608.

(17) Guo, Z.; Chen, G.; Cometto, C.; Ma, B.; Zhao, H.; Groizard, T.; Chen, L.; Fan, H.; Man, W.-L.; Yiu, S.-M.; Lau, K.-C.; Lau, T.-C.; Robert, M. Selectivity Control of CO versus HCOO− Production in the Visible-Light-Driven Catalytic Reduction of CO2 with Two Cooperative Metal Sites. *Nat Catal* **2019**, *2* (9), 801–808. https://doi.org/10.1038/s41929-019-0331-6.

(18) Wang, M.; Torbensen, K.; Salvatore, D.; Ren, S.; Joulié, D.; Dumoulin, F.; Mendoza, D.; Lassalle-Kaiser, B.; Işci, U.; Berlinguette, C. P.; Robert, M. CO2 Electrochemical Catalytic Reduction with a Highly Active Cobalt Phthalocyanine. *Nature Communications* **2019**, *10* (1), 3602. https://doi.org/10.1038/s41467-019-11542-w.

(19) Kaiser, A.; Arndtsen, B. A. Carbonylative C□H Bond Activation. In *The Chemical Transformations of C1 Compounds*; John Wiley & Sons, Ltd, 2022; pp 533–565. https://doi.org/10.1002/9783527831883.ch11.

(20) Allah, T. N.; Ponsard, L.; Nicolas, E.; Cantat, T. Catalytic Challenges and Strategies for the Carbonylation of σ-Bonds. *Green Chem.* **2021**, *23* (2), 723–739. https://doi.org/10.1039/D0GC02343D.

(21) Lukasevics, L.; Grigorjeva, L. Cobalt-Catalyzed Carbonylation of the C–H Bond. *Org. Biomol. Chem.* **2020**, *18* (38), 7460–7466. https://doi.org/10.1039/D0OB01633K.

(22) Evans, D.; Osborn, J. A.; Wilkinson, G. Hydroformylation of Alkenes by Use of Rhodium Complex Catalysts. *J. Chem. Soc. A* **1968**, No. 0, 3133–3142. https://doi.org/10.1039/J19680003133.

(23) Le Berre, C.; Serp, P.; Kalck, P.; Torrence, G. P. Acetic Acid. In *Ullmann's Encyclopedia of Industrial Chemistry*; John Wiley & Sons, Ltd, 2014; pp 1–34. https://doi.org/10.1002/14356007.a01_045.pub3.

(24) Sunley, G. J.; Watson, D. J. High Productivity Methanol Carbonylation Catalysis Using Iridium: The Cativa™ Process for the Manufacture of Acetic Acid. *Catalysis Today* **2000**, *58* (4), 293–307. https://doi.org/10.1016/S0920-5861(00)00263-7.

(25) Meng, Q.; Yan, J.; Wu, R.; Liu, H.; Sun, Y.; Wu, N.; Xiang, J.; Zheng, L.; Zhang, J.; Han, B. Sustainable Production of Benzene from Lignin. *Nat Commun* **2021**, *12* (1), 4534. https://doi.org/10.1038/s41467-021-24780-8.

(26) Machas, M.; Kurgan, G.; Jha, A. K.; Flores, A.; Schneider, A.; Coyle, S.; Varman, A. M.; Wang, X.; Nielsen, D. R. Emerging Tools, Enabling Technologies, and Future Opportunities for the Bioproduction of Aromatic Chemicals. *Journal of Chemical Technology & Biotechnology* **2019**, *94* (1), 38–52. https://doi.org/10.1002/jctb.5762.

(27) Brühne, F.; Wright, E. Benzaldehyde. In *Ullmann's Encyclopedia of Industrial Chemistry*; John Wiley & Sons, Ltd, 2011. https://doi.org/10.1002/14356007.a03_463.pub2.

(28) Eisenberg, R. Photochemical C−H Activation: An Early Story. *Israel Journal of Chemistry* **2017**, *57* (10/11), 932–936. https://doi.org/10.1002/ijch.201700046.

(29) Kunin, A. J.; Eisenberg, Richard. Photochemical Carbonylation of Benzene by Iridium(I) and Rhodium(I) Square-Planar Complexes. *J. Am. Chem. Soc.* **1986**, *108* (3), 535–536. https://doi.org/10.1021/ja00263a045.

(30) Boyd, S. E.; Field, L. D.; Partridge, M. G. Characterization of Organometallic Products from the Photochemical Reaction of Trans-Rh(PMe3)2(CO)Cl with Benzene. *J. Am. Chem. Soc.* **1994**, *116* (21), 9492–9497. https://doi.org/10.1021/ja00100a012.

(31) Gordon, E. M.; Eisenberg, R. The Photochemical Carbonylation of Benzene, and Hydrogenation and Hydrosilation of Benzaldehyde Catalyzed by Ruthenium(O) Complexes. *Journal of Molecular Catalysis* **1988**, *45* (1), 57–71. https://doi.org/10.1016/0304-5102(88)85030-2.

(32) Kläui, W.; Schramm, D.; Peters, W. Photoinduced C–H Activation and Catalytic Carbonylation of Benzene – New Features of a Tris(Pyrazolyl)Methanesulfonato (Tpms) Rhodium(I) Complex. *European Journal of Inorganic Chemistry* **2001**, *2001* (12), 3113–3117. https://doi.org/10.1002/1099-0682(200112)2001:12<3113::AID-EJIC3113>3.0.CO;2-#.

(33) Kunin, A. J.; Eisenberg, Richard. Photochemical Carbonylation of Benzene by Iridium(I) and Rhodium(I) Square-Planar Complexes. *Organometallics* **1988**, *7* (10), 2124–2129. https://doi.org/10.1021/om00100a007.

(34) Khusnutdinova, J. R.; Milstein, D. Metal–Ligand Cooperation. *Angewandte Chemie International Edition* **2015**, *54* (42), 12236–12273. https://doi.org/10.1002/anie.201503873.

(35) Alig, L.; Fritz, M.; Schneider, S. First-Row Transition Metal (De)Hydrogenation Catalysis Based On Functional Pincer Ligands. *Chem. Rev.* **2019**, *119* (4), 2681–2751. https://doi.org/10.1021/acs.chemrev.8b00555.

(36) Elsby, M. R.; Baker, R. T. Strategies and Mechanisms of Metal–Ligand Cooperativity in First-Row Transition Metal Complex Catalysts. *Chem. Soc. Rev.* **2020**, *49* (24), 8933–8987. https://doi.org/10.1039/D0CS00509F.

(37) Tocqueville, D.; Crisanti, F.; Guerrero, J.; Nubret, E.; Robert, M.; Milstein, D.; Wolff, N. von. Electrification of a Milstein-Type Catalyst for Alcohol Reformation. *Chem. Sci.* **2022**, *13* (44), 13220–13224. https://doi.org/10.1039/D2SC04533H.

(38) Kasemthaveechok, S.; Gérardo, P.; Wolff, N. V. Merging Electrocatalytic Alcohol Oxidation with C-N Bond Formation by Electrifying Metal-Ligand Cooperative Catalysts. *Chem. Sci.* **2023**. https://doi.org/10.1039/D3SC03408A.

(39) Sakakura, T.; Sodeyama, T.; Sasaki, K.; Wada, K.; Tanaka, M. Carbonylation of Hydrocarbons via Carbon-Hydrogen Activation Catalyzed by RhCl(CO)(PMe3)2 under Irradiation. *J. Am. Chem. Soc.* **1990**, *112* (20), 7221–7229. https://doi.org/10.1021/ja00176a022.

(40) Rosini, G. P.; Boese, W. T.; Goldman, A. S. Study of the Mechanism of Photochemical Carbonylation of Benzene Catalyzed by Rh(PMe3)2(CO)Cl. *J. Am. Chem. Soc.* **1994**, *116* (21), 9498–9505. https://doi.org/10.1021/ja00100a013.

(41) McLoughlin, E. A.; Matson, B. D.; Sarangi, R.; Waymouth, R. M. Electrocatalytic Alcohol Oxidation with Iron-Based Acceptorless Alcohol Dehydrogenation Catalyst. *Inorg. Chem.* **2020**, *59* (2), 1453–1460. https://doi.org/10.1021/acs.inorgchem.9b03230.

(42) Annen, S. P.; Bambagioni, V.; Bevilacqua, M.; Filippi, J.; Marchionni, A.; Oberhauser, W.; Schönberg, H.; Vizza, F.; Bianchini, C.; Grützmacher, H. A Biologically Inspired Organometallic Fuel Cell (OMFC) That Converts Renewable Alcohols into Energy and Chemicals. *Angewandte Chemie International Edition* **2010**, *49* (40), 7229–7233. https://doi.org/10.1002/anie.201002234.

(43) Anaby, A.; Feller, M.; Ben-David, Y.; Leitus, G.; Diskin-Posner, Y.; Shimon, L. J. W.; Milstein, D. Bottom-Up Construction of a CO2-Based Cycle for the Photocarbonylation of Benzene, Promoted by a Rhodium(I) Pincer Complex. *J. Am. Chem. Soc.* **2016**, *138* (31), 9941–9950. https://doi.org/10.1021/jacs.6b05128.

(44) Zhou, C.; Hu, J.; Wang, Y.; Yao, C.; Chakraborty, P.; Li, H.; Guan, C.; Huang, M.-H.; Huang, K.-W. Selective Carbonylation of Benzene to Benzaldehyde Using a Phosphorus–Nitrogen PN3P–Rhodium(i) Complex. *Org. Chem. Front.* **2019**, *6* (6), 721–724. https://doi.org/10.1039/C8QO00892B.

(45) Hanson, S. K.; Heinekey, D. M.; Goldberg, K. I. C–H Bond Activation by Rhodium(I) Phenoxide and Acetate Complexes: Mechanism of H–D Exchange between Arenes and Water. *Organometallics* **2008**, *27* (7), 1454–1463. https://doi.org/10.1021/om7012259.

(46) Schwartsburd, L.; Iron, M. A.; Konstantinovski, L.; Ben-Ari, E.; Milstein, D. A Dearomatized Anionic PNP Pincer Rhodium Complex: C–H and H–H Bond Activation by Metal–Ligand Cooperation and Inhibition by Dinitrogen. *Organometallics* **2011**, *30* (10), 2721–2729. https://doi.org/10.1021/om200104b.

(47) Monlien, F. J.; Helm, L.; Abou-Hamdan, A.; Merbach, A. E. Mechanistic Diversity Covering 15 Orders of Magnitude in Rates: Cyanide Exchange on [M(CN)4]2- (M = Ni, Pd, and Pt)1. *Inorg. Chem.* **2002**, *41* (7), 1717–1727. https://doi.org/10.1021/ic010917e.